World Conference on Timber Engineering Oslo 2023

EFFECTS OF PANEL DIRECTION, LOAD LEVEL AND AMBIENT HUMIDITY ON THE CREEP OF DOWNSCALED CROSS-LAMINATED TIMBER

Dawei Wang[1], Meizhen Chen[1], Meng Gong[2], Zhuo Cheng[3]

ABSTRACT: The creep behaviour of wood or engineered wood products is an important factor in the consideration of the serviceability of a timber structure. This study evaluated the effect of creep of downscaled cross-laminated timber *(CLT)* specimens by considering panel direction, load level and relative humidity *(RH)*. The test materials were spruce-pine-fir (*SPF*) lumber and polyurethane adhesive. Static bending, one-week creep and four-month creep tests were conducted. It was found that: 1) *CLT* specimens had an average proportional limit *(PL)* of around 3,024 N and 817 N in the "Major-strength" and "Minor-strength" directions, respectively; 2) Panel direction strongly impacted time-dependent deflection, with the "Minor-strength" specimens exhibiting a 2 to 2.5 times as large deflection as the "Major-strength" ones; 3) Load level clearly affected the load-deflection behaviour due to the layup of the specimens; 4) Ambient humidity had a little effect on 7-day creep, but impacted the 4-month mechano-sorptive creep to some degree; and 5) The "Generalized Kelvin" model seemed to be suitable in simulation the creep of the downscaled *CLT* specimens used in this study. The upper limit of the model at 95% confidence level could be a good approach to simulate the creep of the specimens under cyclic *RH*.

KEYWORDS: Cross-laminated timber, Relative humidity, Load level, Panel direction, Creep, Mechano-sorptive behaviour, Modelling

1 INTRODUCTION

The use of cross-laminated timber (*CLT*), an innovative green building material, has gained widespread popularity in recent years, particularly for the construction of mid- and high-rise timber structures. The advanced cross-laminate technology utilized in *CLT* production provides the panels with improved dimensional stability and high in- and out-of-plane stiffness and strength properties, leading to its two-way action capability and enhanced high-strength construction [1]. Additionally, *CLT* offers a cost-effective alternative to traditional building materials such as concrete and steel, as its light weight reduces the size and cost of foundations. The great seismic and fire performance of *CLT* panels further adds to their suitability for use in various building environments [1].

The evaluation of the serviceability of a timber structure requires a thorough understanding of the concept of creep, which can be classified into two types: "pure" creep and mechano-sorptive creep. "Pure" creep is defined as the time-dependent deformation caused by a material under constant load [2], while mechano-sorptive creep is the deformation affected by an interaction between humidity variations and mechanical loading [3]. The creep behaviour of wood is subject to various factors, including temperature, relative humidity (*RH*), grain direction of wood, strength direction of a product, loading condition, member size, and anatomical features of wood. However, the mechano-sorptive creep of *CLT* is specifically influenced by the ambient temperature and humidity when it happens [2]. Despite its importance, research on the mechano-sorptive creep of *CLT* remains limited.

In the early stage of research, the evaluation of creep behaviour in wood materials was primarily conducted through experiments utilizing both small clear wood specimens and full-scale timber products [4-5]. These wood materials were analysed by utilizing rheological and viscoelastic theories, leading to a thorough understanding of their creep behaviour. Under variable temperature and moisture conditions, the time-dependent behaviour of wood is highly complex [6]. Phenomenological studies, similar to those conducted by Schniewind [4], were performed to investigate the impact of environmental factors on creep behaviour, with results obtained for both constant and varying conditions during the course of an experiment. Subsequent studies indicated that creep was often more vulnerable to changes in temperature, moisture content (*MC*), and physical ageing than its elastic properties [2, 7]. Since then, efforts have been made on the studies that included creep by considering multiple influencing factors such as humidity effect, as well as the development of creep models. Over the past several decades, there has been a remarkable advancement in the study of the viscoelastic properties of wood. This has been achieved largely through the innovation and improvement

[1] Dawei Wang, Faculty of Forestry and Environmental Management, University of New Brunswick, Canada, dwang12@unb.ca
[1] Meizhen Chen, Faculty of Forestry and Environmental Management, University of New Brunswick, Canada, meizhen.chen@unb.ca
[2] Meng Gong, Wood Science and Technology Centre, University of New Brunswick, Canada, mgong@unb.ca
[3] Zhuo Cheng, Off-site Construction Research Centre, University of New Brunswick, Canada, zcheng2@unb.ca.

https://doi.org/10.52202/069179-0071

of testing methods, the collection of experimental data, and the formation of rheological models. These progresses have occurred in parallel with the rapid expansion of the wood-based products industry and uses of wood-based products in construction, leading to a corresponding invention and development of various types of engineered wood products (*EWPs*), such as *CLT*. Bengtsson [8] conducted a third-point bending test using Norway spruce (*Picea abies*) specimens and observed that *MC* and density strongly influence the creep behaviour of timber. The study also demonstrated a strong correlation between the relative creep and modulus of elasticity. O'Ceallagh et al. [9] conducted third-point bending tests under constant stress levels using Sitka spruce (*Picea sitchensis*) for 75 weeks to investigate the mechano-sorptive creep behaviour of unreinforced and fiber-reinforced polymer (*FRP*) plate-reinforced glued laminated timber beams with the variable *RH* ranging from 65±5% to 90±5%. The results indicated that variable *RH* values significantly influenced creep behaviour. The first *RH* cycle caused a statistically significant reduction in both total and creep deflection. Takanashi et al. [10] conducted long-term out-of-plane bending tests on full-scale seven-layer Japanese larch (*Larix kaempferi*) *CLT* panels and estimated a mean relative creep of 1.49 after 50 years using a power-law function developed by Holzer [6]. The authors also recommended avoiding *CLT* products made from Japanese larch when subjected to loading levels of 70% or more. Hunt [11] proposed a unified approach to modelling the creep behaviour of Ponderosa pine (*Pinus ponderosa*), who was aimed at developing a mathematical model that could accurately predict the long-term deformation of wood under varying stress levels and environmental conditions. He reported that the full extent of the mechano-sorptive effect would require the timber to reach equilibrium moisture content (*EMC*) under new environmental conditions. Therefore, multiple changes of *RH* in full-scale tests may yield inaccurate results. Due to the lack of a harmonized standard for examining the mechano-sorptive effect in *EWPs*, the duration of creep tests and *RH* cycles vary significantly between test programs. Liu et al. [4] analysed different models for simulating creep in laminated veneer lumber products by using third-point bending test under short- and long-term constant loading and found that the modified Burger model provided good simulation. Cai et al. [12] used the specimens of southern pine (*Pinus spp.*) to give two sets of tests for creep and creep recovery, which presented new models for creep and creep recovery, which could be well fitted to both primary and secondary stages of creep deformation using modified power-law functions.

This study was aimed at investigating and simulating the creep behaviour of *CLT* using the downscaled specimens by considering panel direction, load level and ambient humidity.

2 MATEIRALS AND METHODS

2.1 MATERIALS AND SPECIMENS

Downscaled *CLT* specimens consisting of three-layers were produced using 2×6 No.2 Spruce-Pine-Fir (*SPF*) with moisture-activated polyurethane adhesive (*PUR*) with reference to the standard ANSI/APA PRG 320 and *CLT* Handbook [13-14]. The dimensions of each lamination were 11 mm in thickness, 63 mm in width, and 710 mm in length. The dimensions of each three-layer downscaled *CLT* were 33 mm in thickness, 63 mm in width, and 710 mm in length. Two types of three-layer specimens were fabricated, taking into account the panel direction, i.e., "Major-strength" and "Minor-strength" directions. Table 1 provides the specimen information, in which the notation "S" stands for static bending, "A" for "Major-strength" direction, "O" for "Minor-strength" direction, and "C" and "D" for one-week and four-month creep tests. The manufacturing process is illustrated in Fig. 1. The test specimens were conditioned at 20°C and 65% *RH* until they achieved a constant *MC* of 12%.

Table 1: *Groups and sets labelling of specimens.*

Tests		Panel direction	Load level	RH level	Groups/ sets
Static (S)		Major	/	/	SA
		Minor	/	/	SO
Creep	7-day (C)	Major	30%	65%	CA1
				30%	CA2
			60%	65%	CA3
				30%	CA4
		Minor	30%	65%	CO1
				30%	CO2
			60%	65%	CO3
				30%	CO4
	4-month (D)	Major	30%	30-65% Cyclic	DA1
			60%		DA2
		Minor	30%	30-65% Cyclic	DO1
			60%		DO2

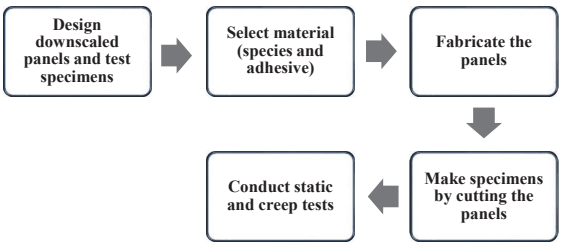

Figure 1: *Design and manufacturing of downscaled CLT.*

2.2 METHODS

2.2.1 Static bending test

The third-point bending tests were conducted at a loading rate of 5 mm/min and a span ratio of 16.4 with reference

to ASTM D198–15 [15] with an aim at determining the limits of proportion (*PL*s) of the *CLT* specimens in the "Major-strength" and "Minor-strength" directions, Fig. 2. A Linear variable differential transformer (*LVDT*) was used to measure the deflection at the mid-span of each specimen, Fig. 2.

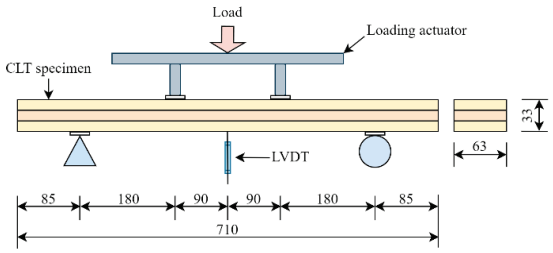

***Figure 2**: Static bending test setup (Unit-mm).*

2.2.2 One-week creep test

A third-point bending setup was employed to conduct a one-week creep test in a conditioning chamber, with a temperature of 20±1°C, Figs. 3 and 4. Two types of specimens were used, "Major-strength" and "Minor-strength". Two levels of *RH* were employed, 30±5% and 65±5%. Two load levels were set at 30% and 60% of the *PL*. The target load was achieved by placing steel plates on each specimen, Fig. 3.

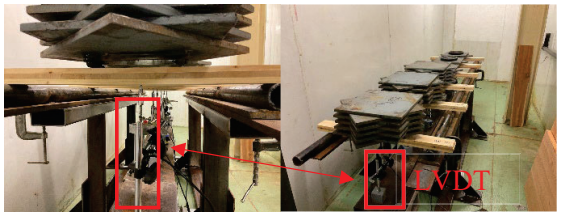

***Figure 3**: Creep test setup with an LVDT at the mid-span of each specimen.*

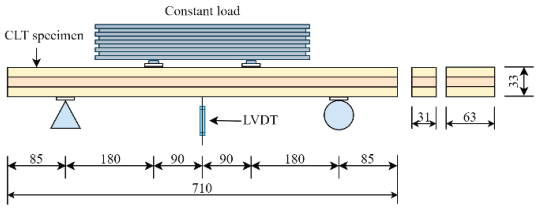

***Figure 4**: Creep test setup (Unit-mm).*

The deflection at the mid-span of each specimen was recorded using an *LVDT* connected to a data logger with a frequency of 1 Hz. In order to safely and efficiently apply the constant load up to 60% *PL* on those specimens, a given *CLT* specimen was ripped into two narrow specimens along the middle line, see the two different cross sections in Fig. 4. The load applied on each narrow specimen (i.e., after ripping) was half of that on the specimen of full width (i.e., before ripping). The loading duration was of 7 days. Six specimens (three specimens per type) were tested at a given load level and *RH*, generating a total of 24 specimens in this phase of testing.

2.2.3 Four-month mechano-sorptive creep test

The four-month mechano-sorptive creep tests were carried out using the same setup as that in the one-week one, Figs. 3 and 4. The load level and panel direction considered were the same as those of 7-day creep tests. The tests were conducted under a constant temperature of 20±1°C in a conditioning chamber with two levels of *RH* (i.e., 30±5% and 65±5%) with an interval of 7 days. The test specimens for the four-month mechano-sorptive creep tests were obtained from the same specimens that had been subjected to a 7-day loading duration and recovered in the chamber for about one year in a conditioning chamber of a temperature of 20°C and 65% *RH*. This allowed the completely release of any residual stress in a specimen. The specimens at 30% *PL* were completed a 4-month mechano-sorptive creep. However, the specimens at 60% *PL* were only terminated to 2 months because of the relatively large deflection that caused a specimen to fracture and/or collapse.

2.2.4 Modelling

Great efforts on modelling the creep behaviour of wood and wood composites have been made [16]. Classical models have been developed that can provide a meaningful approximation of the time-dependent deformation of wood, which offer valuable insights into the mechanical behaviour of wood and wood composites. These models are typically based on a combination of a spring(s) and a Newtonian dashpot(s), representing the elastic and viscoelastic nature of a composite such as wood [12]. The models such as the "Maxwell" model, "Kelvin" model, "Generalized Kelvin (*GK*)" model, and "Burger (*B*)" model are commonly used to describe the mechanical response of viscoelastic materials and involve the arrangement of elastic and viscous elements in either series or parallel configurations [2, 16-17].

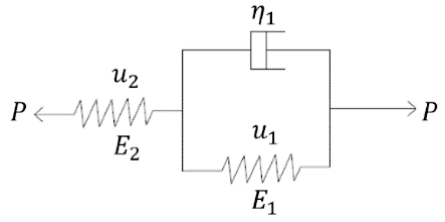

***Figure 5**: "Generalized Kelvin" model [2].*

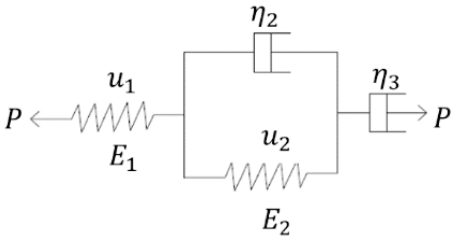

***Figure 6**: "Burger" model [2].*

https://doi.org/10.52202/069179-0071

This study adopted the "*GK*" model and "*B*" model to simulate the creep behaviour of the downscaled *CLT* specimens. The "*GK*" model was chosen due to that it is a derivation from the widely used "Kelvin" model, which can accurately represent the delayed elastic component of a material. The "*B*" model was selected due to its simplicity as well as the model parameters are expressed on a unit basis, relating time-dependent stress-strain behaviour to the modulus of elasticity and rigidity and to the coefficients of the viscosity of a composite [2].
These two models are illustrated in Figs. 5 and 6, in which, E is the modulus of elasticity of a spring; η is the viscosity coefficient of a dashpot; P is the force applied; τ is the relaxation-time constant which is η/E; u is the displacement; t is creep time [4].

***Table 2**: Two creep model equations.*

Creep Model	Creep Equation
"Generalized Kelvin" model	$u = -Ae^{-Bt} + D$
"Burger" model	$u = -Ae^{-Bt} + Ct + D$

Table 2 gives the simplified forms (equations) of two creep models. Where, $A = P_1/E_1$, $B = 1/\tau_1$, and $D = P_1/E_1 + P_2/E_2$, in "*GK*" model; $A = P/E_2$, $B = 1/\tau_2$, $C = P/\eta_3$ and $D = P/E_1 + P/E_2$, in "*B*" model.

3 RESULTS AND DISCUSSION

3.1 STATIC BENDING TEST

Fig. 7 illustrates the load-deflection curves of two groups. Groups SA and SO represent the groups in the "Major-strength" and "Minor-strength" directions. It can be found most specimens failed in a brittle way. It can also be found that one specimen in group SA exhibited an abnormal response, which could be due to the existence of imperfects during manufacturing of specimens such as lack of adhesive causing delamination between laminations. Consequently, this specimen was eliminated from the data analysis. The average peak loads of groups SA and SO were approximately 6,094 N and 1,249 N, respectively. The average *PL* values of groups SA and SO were around 3,024 N and 817 N, respectively. The average stiffness of group SA was approximately 610 N/mm, which was approximately 10 times larger than that of group SO.
Table 3 summarizes the test results of two groups including stiffness, *PL* and P_{max}, plus the deflection at P_{max}. It is not surprising that the group SA (i.e., the "Major-strength" group) exhibit higher strength and stiffness. The deflection at the peak load is around 11 mm, which is about 35% lower than that of the group SO. The maximum bending capacity of the group SA was about 3 times greater than that of the group SO. Subsequent to the static bending test, two load levels were then determined, based on the *PL,* to be 30% *PL* and 60% *PL* for the "Major-strength" and "Minor-strength" groups for the following creep tests.

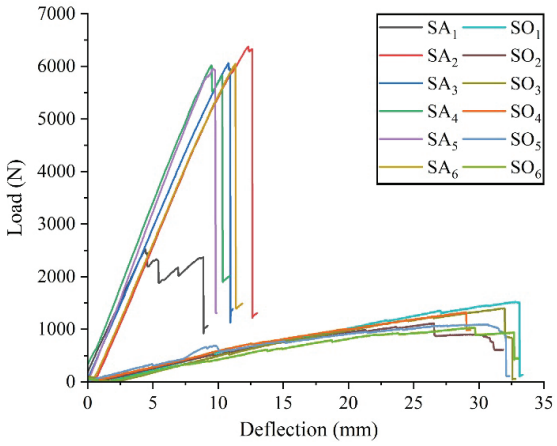

***Figure 7**: Load-deflection curves in the "Major-strength" and "Minor-strength" directions.*

***Table 3**: Mean properties of downscale CLT specimens under the static bending tests (Note: Numbers in parentheses are standard deviations).*

Property	Mean	
	Group SA	**Group SO**
Stiffness (N/mm)	610 (4)	60 (0)
PL (N)	3,024 (431)	817 (238)
P_{max} (N)	6,094 (163)	1,249 (196)
Deflection (mm)	11.36 (1.16)	32.13 (1.46)

3.2 ONE-WEEK CREEP TEST

Fig. 8 was used to illustrate the creep deflections of all specimens under two-panel directions, two load levels, and two *RH* conditions, with each curve representing the average deflection-time response of the corresponding set. It can be obviously seen that the load level had a significant impact on the creep. Each curve consists of two stages, namely the initial creep stage and the steady creep stage. The maximum load applied on a specimen in this study was 60% of *PL*, the accelerated creep stage did not appear in the 7-day creep test, which suggests that the maximum deflection had not exceeded the specimen's deflection limit and caused failure in the 7-day [18]. Thus, only the initial creep stage and steady creep stage were discussed and simulated in 7-day creep test. It can be discovered that the eight sets largely conformed to the general law of creep.
It can be found from Fig. 8 that 1) For the panel direction: the average deflection reached by the "Minor-strength" groups (sets CO1 and CO2) loaded at 30% *PL* are approximately 11.85 mm, which is 2.2 times larger than that made by the "Major-strength" groups (sets CA1 and CA2). For the sets loaded at 60% *PL*, the average deflection of the "Minor-strength" groups (sets CO3 and CO4) was approximately 21.83 mm at 172 hours, which is 2.71 times larger than that of the "Major-strength" groups (sets CA3 and CA4) with a deflection of 8.07 mm.

https://doi.org/10.52202/069179-0071

This is well in agreement with the findings by He et al. [19]; 2) For the load level: "Major-strength" groups bewteen sets CA1-2 and CA3-4 were compared, which revealed a small difference in deflection values at the termination of testing, with average values of 5.39 mm and 8.07 mm, respectively. "Minor-strength" groups bewteen sets CO1-2 and CO3-4 exhibited a much larger difference with the average values of 11.83 mm and 21.83 mm. Especially, set CO3 is about 22.74 mm, the maximum deflection set in 7-day creep test, which is 1.93 times that of set CO1 with a deflection of 11.81 mm at the time of 172 hours; 3) For the *RH*: A comparison made between two *RH*s revealed that the deflection in higher *RH* sets was greater than lower *RH* sets, while keeping other conditions unchanged. This observation can be attributed to the difference in the *MC* of the specimens used, which well aligns with other findings [2, 7-8].

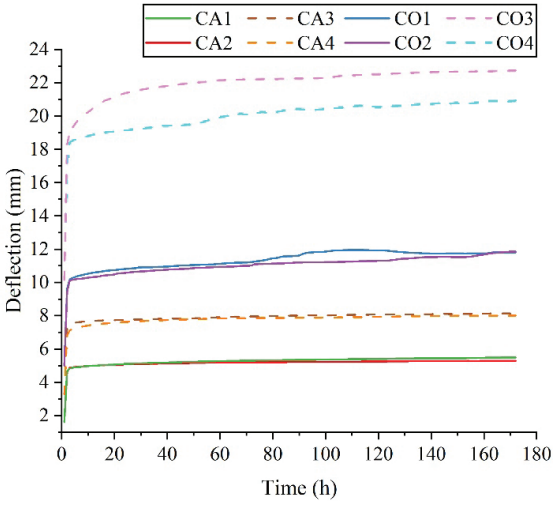

***Figure 8**: Average 7-day creeps of eight sets tested.*

3.3 FOUR-MONTH MECHANO-SORPTIVE CREEP TEST

Fig. 9 depicts the 4-month mechano-sorptive creeps of all sets under two-panel directions, two load levels, and cyclic *RH* ranging from 30% to 60% with a time interval of 7 days. Each curve represents the average deflection-time response of a given set. It can be clearly seen that all setting factors mentioned above had a significant effect on the creep of the specimens tested. It can be discovered that sets DA1 and DO1 largely conformed to the general law of mechano-sorptive creep.

Fig. 9 shows that sets DA2 and DO2, which were loaded at 60% *PL*, had to be halted at the time of about 900 hours due to the collapse of two "Major-strength" *CLT* specimens and the destruction of one "Minor-strength" *CLT* specimen. Based on Fig. 9 and Table 3, the initial deflections of sets DA1-2 and DO1-2 were 1.61 mm and 3.27 mm in the "Major-strength" direction and were 4.99 mm and 10.14 mm in the "Minor-strength" direction, as presented in Table 4. Those initial deflections were using average static bending test data. Additionally, Table 4 presented the total deflection that the specimens experienced on average, derived by considering initial deflection and maximum creep deflection together. Remarkably, the deflections of sets DA2 and DO2 at the end of loading were 9.64 mm and 28.88 mm, respectively, which almost reached the ultimate deflection at a given direction, Table 3, namely, 11.36 mm or 32.13 mm for the "Major-strength" or "Minor-strength" direction. The specimens in sets DA2 and DO2 were speculated to have exceeded the bending yield point and created a high creep deflection causing the specimens to collapse or destroy during the test. Therefore, only the 4-month mechano-sorptive creeps of sets DA2 and DO2, i.e., those subjected to 60% *PL* load level, were excluded from the data analysis and discussion in this study.

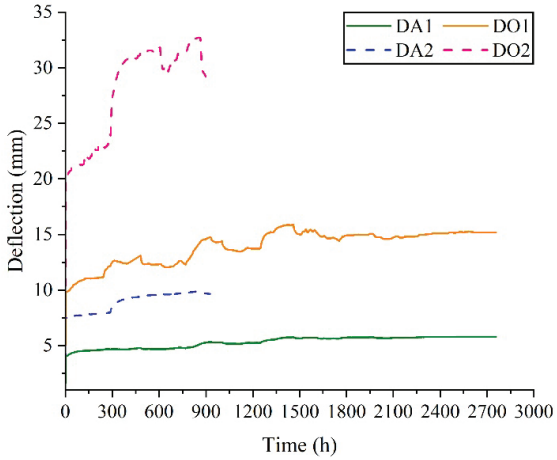

***Figure 9**: Average four-month mechano-sorptive creeps of four sets tested.*

***Table 4**: Average deflections of the specimens tested under the cyclic RH (Unit-mm).*

Test sets	Initial deflection	Deflection at the end of testing	Total deflection
DA1	1.61	4.18	5.79
DA2	3.27	6.37	9.64
DO1	4.99	10.20	15.19
DO2	10.14	18.74	28.88

It can be discovered from Fig. 9 that the panel direction significantly affected the creeps of the specimens under 30% *PL*. Specifically, set DO1 exhibited a deflection of approximately 14.59 mm at 900 hours, which is 277% larger than set DA1 that had a deflection of 5.27 mm. As the testing of sets DA1 and DO1, the deflection curve gradually increased from the initial stage. The sets DA1 and DO1 reached the maximum discrepancy in deflection at 1459 hours, with deflections of 5.76 mm and 15.90 mm, respectively. At the steady stage, which is at 2755 hours, the deflection was 5.79 mm and 15.19 mm for the sets DA1 and DO1, respectively. It is apparent that the

https://doi.org/10.52202/069179-0071

deflection of set DO1 was 262% larger than that of set DA1 to a large degree.

Fig. 10 illustrates the changes in temperature and *RH* values during the 4-month mechano-sorptive creep tests. It can be found thatt temperature was well mainained at 20°C, while *RH* was not well controled at the preset range, i.e., from 30±5% to 65±5%, due to the out-of-control of the chamber during the creep test duration. Fig. 9 indicates that significant increases in deflection were observed at approximately 300, 900, and 1300 hours. The increase in deflection of set DO1 ranged from 12.49 to 15.13 mm, while that of set DA1 was only 4.68 to 5.49 mm when the *RH* increased from 30% to 70% at the times of about 300, 900 and 1300 hours.

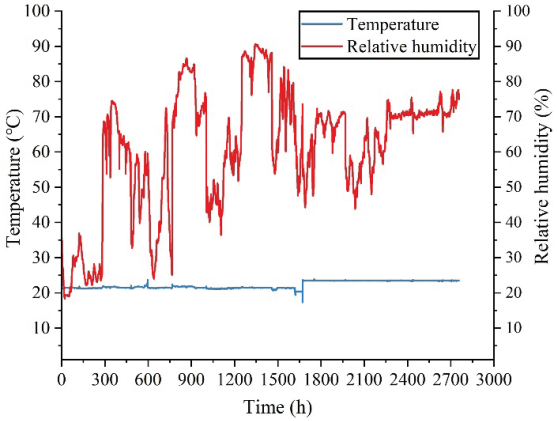

***Figure 10**: Changes in temperature and RH during the creep tests of sets DA1 and DO1.*

There are some shortcomings existed during the mechano-sorptive creep tests in this study, resulting in unsatisfactory results. Firstly, the application of a 60% *PL* load level for the long-term creep test was inappropriate (sets DA2 and DO2) since it could cause a relatively large deflection at 900 hours, which exceeded that at the maximum load under the static tests. Secondly, the *RH* in the conditioning chamber used was not well controlled to some degree as planned. Thirdly, the 4-month duration of the mechano-sorptive creep test could not be sufficient, which was due to the duration (only 1 year) of a project-based master's student's study. Finally, the downsized *CLT* specimens were not good enough to represent the full size *CLT* panels. Hence, there is a need for further research to overcome these shortcomings.

3.4 MODELLING

The "*GK*" model and "*B*" model were selected to simulate the creep of downscaled *CLT* specimens loaded at 30% *PL* in this study. The Curve Fitting Function in Origin software developed by OriginLab Corporation was used to determine the parameters in each model by the non-linear fitting method. The fitting results are provided in Table 5, and Figs. 11 to 12. The R-square values of over 0.85 suggests that both models well fit the experimental data and seems the fitting curve of the "Major-strength" set is slightly better than that of the "Minor-strength" one at a given model. The 95% of prediction bands (filled colour) of each model are plotted in Figs. 11 and 12 as well. Considering the fluctuation of time-dependent deflection due to the cyclic *RH*, the upper limit of 95% confidence level is employed to build "*GK*" model or "*B*" model, which reflects the worst-case scenario for downscaled *CLT* specimens used in this study in a given direction. The creep models developed in this study are given in Table 6.

***Table 5**: Determination of model parameters based on the 4-month creep test results of two sets (DA1 and DO1) in both "Major-strength" and "Minor-strength" directions.*

Sets	Model	Parameters				R-Square
		A	*B*	*C*	*D*	
DA1	GK	1.9317	0.0007	/	6.1452	0.9235
	B	0.2452	-0.0008	0.0012	4.5253	0.9384
DO1	GK	5.4571	0.0013	/	15.4085	0.8786
	B	13.6279	0.0006	-0.0022	23.7686	0.8842

The deflections of specimens DA1 and DO1 at 3 months, 6 months, 1 year, 10 years, and 50 years can be predicted using the models developed above, which are listed in Table 6. It can be found that the "*GK*" model could produce more reasonable results than the "*B*" model based on the data in this study. Also, it could be discovered that the deflections predicted by the "*GK*" model become a constant after 1 year. This suggests that a duration of 1 year, or even 6 months, could be good enough for building a creep mode for *CLT* specimens. However, such a speculation requires further verification. Also, a more complex model should be developed by considering panel direction, load level and relative humidity.

https://doi.org/10.52202/069179-0071

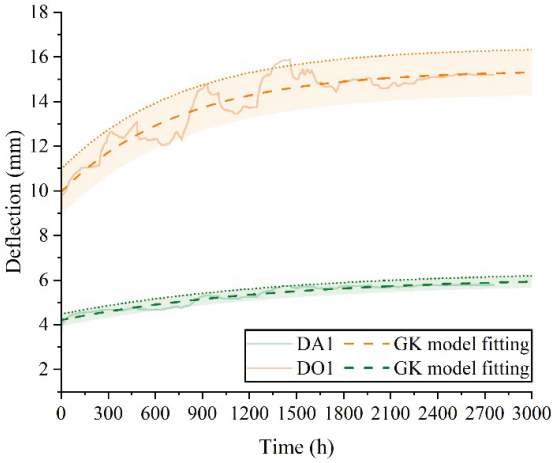

***Figure 11**: "GK" models and prediction bands at 95% confidence level for 4-month mechano-sorptive creep.*

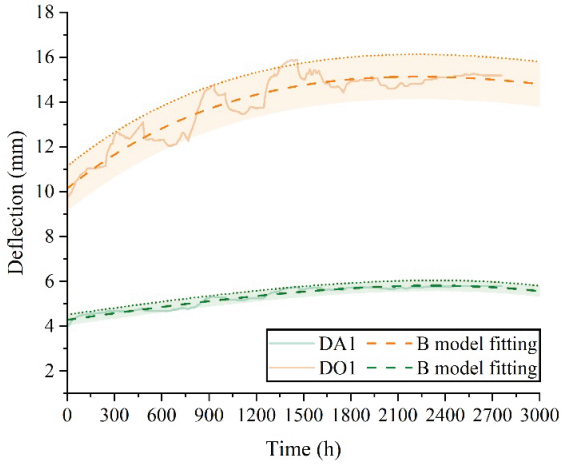

***Figure 12**: "B" models and prediction bands at 95% confidence level for 4-month mechano-sorptive creep.*

***Table 6**: Creep models and predicted deflections at given times.*

Set	Model	Equation	Deflection (mm)				
			Month 3	Month 6	Year 1	Year 10	Year 50
DA1	GK	u=−1.9319$e^{-7.3109t}$ +6.4080	6.01	6.33	6.40	6.41	6.41
	B	u=−0.2518$e^{0.0008t}$+0.0012t+4.7672	6.03	2.71	-216.19	-1.09×10^{29}	-3.82×10^{147}
DO1	GK	u= −5.4555$e^{-0.0013t}$+16.4243	16.10	16.40	16.42	16.42	16.42
	B	u= −13.5727$e^{-0.0006t}$−0.0022t+24.7067	16.12	14.20	5.59	-165.55	-926.60

4 CONCLSUIONS

Based on the above analysis and discussion, the following conclusions could be drawn:

(1) The *CLT* specimens had average *PL*s of approximately 3,024 N and 817 N in the "Major-strength" and "Minor-strength" directions, respectively.

(2) The results of the one-week creep tests indicated that the panel direction of *CLT* specimens was the most influencing factor on their creep behaviour, with the "Minor-strength" specimens exhibiting an average creep deflection being 2 to 2.5 times larger than that of the "Major-strength" ones. The initial deflection of those specimens loaded at a level of 60% *PL* was approximate twice as large as that at a level of under 30% *PL*. The effect of *RH* on the creep of the specimens during the one-week loading was found to be less significant than that of the panel direction or load level.

(3) The four-month mechano-sorptive creep results showed that the panel direction, load level and *RH* all played a critical role in contribution to the creep of downscaled *CLT* specimens. A reduction of *RH* to 30% from 65% reduced the creep to some degree.

(4) The "Generalized Kelvin" model seemed to be suitable in simulation the creep of the downscaled *CLT* specimens used in this study. The upper limit of the model at 95% confidence level could be a good approach to simulate the creep of the specimens under cyclic *RH*.

ACKNOWLEDGEMENTS

The authors wish to acknowledge the financial support from the New Brunswick Innovation Research Chair Initiative Program by the New Brunswick Innovation Foundation (Canada), the 3+1+1 Program between the University of New Brunswick (Canada) and Nanjing Forestry University (China), and the technical support from the University of New Brunswick's Wood Science Technology Centre, Canada.

REFERENCES

[1] Gong M. Lumber-based mass timber products in construction. In Timber Buildings and Sustainability. IntechOpen. 10 Lower Thames Street, London, UK. 2019.

[2] Bodig J., & Jayne B.A. Mechanics of wood and wood composites. Van Nostrand Reinhold. New York. 1982.

[3] Martensson A. Creep behavior of structure timber under varying humidity conditions. Journal of Structure Engineering, University of Lund, Lund, Sweden. 1994.

[4] Liu Y., Tang S., Sun X., Gao Z., Gong M. Testing and modeling of creep of poplar laminated veneer lumber beams. World Conference on Timber Engineering. Santiago, Chile. 2020.

https://doi.org/10.52202/069179-0071

[5] Schniewind P. Recent progress in the study of the rheology of wood. Wood Science and Technology, 2(3): 188-20. 1968.
[6] Holzer S., Loferski J., and Dillard D. A review of creep in wood: concepts relevant to develop long-term behavior predictions for wood structures. Wood and Fiber Science, pp: 376-392. 1989.
[7] Armstrong L.D., and Christensen G.N. Influence of moisture changes on deformation of wood under stress. Nature, 191(4791), 869-870. 1961.
[8] Bengtsson C. Mechano-sorptive bending creep of timber-influence of material parameters. Holz als Roh-und Werkstoff, 59(4), 229-236. 2001.
[9] O'Ceallagh C., Sikora K., McPolin D., and Harte A. Mechano-sorptive creep in reinforced glulam. World Conference on Timber Engineering. Seoul, Republic of Korea. 2018.
[10] Takanashi R., Ohashi Y., Ishihara W., and Matsumoto K. Long-term bending properties of cross-laminated timber made from Japanese larch under constant environment. Journal of Wood Science, 67(1), 1-10. 2021.
[11] Hunt D.G., A unifed approach to creep of wood. Proc. R. Soc. London Ser. a-Mathematical Phys. Eng. Sci. 455 4077–4095. 1999.
[12] Cai Z., Fridley K.J., Hunt M.O., and Rosowsky D.V. Creep and creep-recovery models for wood under high stress levels. Wood and Fiber Science, 425-433. 2002.
[13] APA -The Engineered Wood Association. Standard for Performance-Rated Cross Laminated Timber, ANSI/APA PRG 320. Tacoma, WA, USA. 2019.
[14] Karacabeyli E., & Gagnon. Introduction to cross-laminated timber (Chapter 1). Cross-laminated Timber (CLT) Handbook. FPInnovations. Pointe-Claire, Quebec, Canada. 2019.
[15] American Society for Testing and Materials (ASTM) International. Standard test methods of static tests of lumber in structural sizes. Designation: D198-15, ASTM International, West Conshohocken, PA, USA. 2015.
[16] Gittus J. Creep, viscoelasticity, and creep fracture in solids. John Wiley and Sons, Inc., New York, NY. Chapter 7. 1975.
[17] Hanhijärvi A. Computational method for predicting the long-term performance of timber beams in variable climates. Materials and Structures, 33, 127-134. 2000.
[18] Peng H., Jiang J., Zhan T., Lü J. A Review of Pure Viscoelastic Creep and Mechano-Sorptive Creep of Wood. Scientia Silvae Sinicae, 52(4): 116-126. 2016. (in Chinese)
[19] He M., Sun X., and Li Z. Bending and compressive properties of cross-laminated timber (CLT) panels made from Canadian hemlock. Construction and Building Materials. 185, 175-183. 2018.